2020-01-1063 Published 14 Apr 2020

Further Experiments on the Effect of Bulk In-Cylinder Temperature in the Pressurized Motoring Setup Using Argon Mixtures

Carl Caruana and Mario Farrugia University of Malta

Gilbert Sammut Jaguar & Land Rover

Emiliano Pipitone University of Palermo

Citation: Caruana, C., Farrugia, M., Sammut, G., and Pipitone, E., "Further Experiments on the Effect of Bulk In-Cylinder Temperature in the Pressurized Motoring Setup Using Argon Mixtures," *SAE Int. J. Advances & Curr. Prac. in Mobility* 2(4):2142-2155, 2020, doi:10.4271/2020-01-1063.

This article is from WCX™ 2020 SAE World Congress Experience.

Abstract

Mechanical friction and heat transfer in internal combustion engines have long been studied through both experimental and numerical simulation. This publication presents a continuation study on a Pressurized Motoring setup, which was presented in SAE paper 2018-01-0121 and found to offer robust measurements at relatively low investment and running cost. Apart from the limitation that the peak in-cylinder pressure occurs around 1 DegCA BTDC, the pressurized motoring method is often criticized on the fact that the gas temperatures in motoring are much lower than that in fired engines, hence might reflect in a different FMEP measurement. In the work presented in SAE paper 2019-01-0930, Argon was used as the pressurization gas due to its high ratio of specific heats. This allowed to achieve higher peak in-cylinder temperatures which close further the gap between fired and motored mechanical friction tests. In 2019-24-0141, Argon was mixed in different proportions with Air to synthesize gases with different ratios of specific heats in the aim of observing any abrupt transitions in the FMEP with different peak in-cylinder temperatures. In this publication, a higher loading test matrix to that published in 2019-24-0141 is presented, with an engine speed ranging from 1400 rpm to 3000 rpm and ratios of specific heats varying from that of Air ($\gamma = 1.4$) to that of Argon ($\gamma = 1.67$). The peak in-cylinder pressure was kept at a constant 103 bar. Results obtained in this work strengthen further the observations made in 2019-24-0141; where the measured FMEP is found to be insensitive to the different peak in-cylinder temperatures. In this study, a fast-response thermocouple of the eroding type was also fitted in the combustion chamber and gas-wall interface temperature histories were recorded. The transient heat flux was also computed through a spectral analysis and reported in this publication.

Introduction

Regulations on internal combustion engine efficiency and emissions have become increasingly stringent which call for more rigorous experimental testing and engine simulation. Experimental testing, which is known to be fundamental for engine simulation modeling is becoming increasingly expensive for the automotive industry; hence methods of testing which give robust results at lesser expense are sought. Two of the most commonly discussed parasitic losses in internal combustion engines are mechanical friction and wall heat transfer.

This publication is a result of a continuation study on a testing method for both mechanical friction and heat transfer. This method is known as 'Pressurized Motoring' or 'Motoring with External Charging'. With this motored method, the intake system of the engine is pressurized which in turn results in peak in-cylinder pressures comparable to that in fired engines. Such method allows a reliable determination of the FMEP due to the fact that both the IMEP and BMEP quantities are small and comparable in magnitude to the FMEP. This results in a small error propagation on the FMEP, especially when compared to that in fired testing [1] Early publications suggesting the use of the Pressurized Motoring date back to 1963 [2], both for understanding mechanical friction and heat transfer. At University of Malta, the Pressurized Motoring method has been equipped with a 'shunt pipe' to recirculate the exhausted air back to the intake [3]. This eliminates the need for a large air compressor, since the make-up air required would be only compensating for the blow-by losses.

Further research at the same university also focused on utilizing Argon [4] and mixtures of Air and Argon [5] to raise the in-cylinder gas temperature in the aim of bridging further the gap between the pressurized motored and fired engine testing and address one of the heavily criticized limitations of the pressurized motoring method. Such work showed no

measurable difference in FMEP with varying the peak bulk gas temperatures. In the work reported in [5], the engine was run from 1400 rpm to 3000 rpm at a constant peak in-cylinder pressure of 84 bar with gas mixtures having ratios of specific heats equal to 1.4, 1.5, 1.6 and 1.67.

In this work, another testing campaign was conducted ranging from 1400 rpm to 3000 rpm, at 103 bar peak in-cylinder pressure and similar gas ratios as that tested in [5]. The aim of this testing campaign was to investigate further the dependency of FMEP on bulk in-cylinder temperature at another load condition, in the hope of increasing the confidence in the conclusion made in the earlier publication [5] through more experimental evidence. Additionally, in this work a transient, erodible fast response thermocouple was fitted in-place of the OEM injector to measure the gas-wall interface temperature with both Air and Argon as the working gas. This was aimed at providing data for exploring friction effects, possibly due to lubrication behavior at high in-cylinder temperatures, as well as giving an indication of heat flux out of the cylinder of a pressurized motored engine.

FIGURE 1 Schematic of the pressurized motoring setup. The engine in the schematic is shown in cross-flow for diagram clarity, however actual setup has both the intake and exhaust on same side of the engine (making the shunt pipe easier to implement)

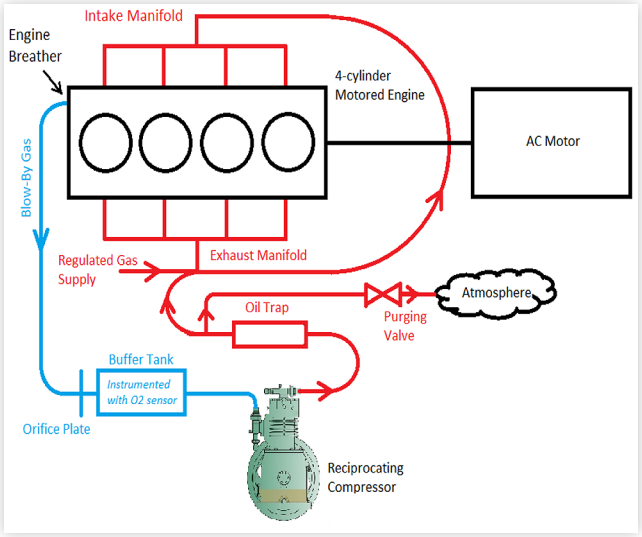

Apparatus

The experimental setup used in this work consists of a 2.0 L, High-Pressure Direct Injection (HDi) engine with a static compression ratio of 18:1. The engine was coupled to an 18 kW AC electric motor, driven with a variable frequency drive (VFD). The setup allowed testing at speeds up to 3000 rpm and 120 bar peak in-cylinder pressure. The intake and exhaust manifolds of the engine were connected through an unrestrictive shunt pipe of internal diameter 55 mm, having a 270° bend of 60 cm diameter. The full specifications of the engine tested are given in Table 1. A schematic of the setup is also given in Figure 1.

In this work, the intake system of the engine was pressurized with pure Air, having a ratio of specific heats (γ) of 1.4, pure Argon with $\gamma = 1.67$ and two other gases synthesized from a mixture of Air and Argon, aimed at having ratios of specific heats of 1.5 and 1.6. The peak in-cylinder pressure during this testing campaign was kept constant and equal to 103 bar, representing around 83% of maximum engine load. Throughout this work, the engine was instrumented with an AVL un-cooled Piezo-electric in-cylinder pressure transducer (GH14P, Serial No. 160506). A 3600 pulse-per-revolution (ppr) crankshaft encoder was used as the clock source for the National Instruments PCI-6251 data acquisition system with a maximum sampling capability of 1 MS/s. The in-cylinder pressure data presented in this paper was referenced to the true TDC of the piston to ±0.1 DegCA. This was possible through the use of an AVL 428 TDC capacitive probe, shown in Appendix Figure. The brake torque required to drive the engine was measured through an S-beam loadcell, connected to a moment arm fixed to the swiveling AC motor.

Several thermocouples were installed on the engine, locations include: shunt pipe intake and exhaust sides, crankcase, coolant jacket and blow-by breather. During the 103 bar testing, a 3 mm diameter ungrounded K-type thermocouple was fitted in the cylinder of the instrumented engine (cylinder 1 - timing belt side). This thermocouple is electrically isolated and was fitted such that its tip is around 1 mm away from the piston when at TDC. The K-type thermocouple used (Part Number: OMEGA CASS-18U-12) is shown in the Figure in Appendix section.

For some of the tested setpoints, an erodible Nanmac E-type transient thermocouple (Serial Number: 65799-1-001) was fitted in place of the OEM injector to have a crank-resolved indication of the gas-wall interface temperature [6, 7]. The erodible thermocouple used in this study (shown in Appendix figure) is made up of two thin thermocouple alloys in ribbon form, separated by a 5μm Mica sheet from each other. Two other Mica sheets isolate the thermocouple alloys on each side and the five layer construction is sandwiched between two Zirconia split-tapered inserts. The entire assembly is pressed into a Stainless Steel ANSI304 ∅1/8" tube and ground flat at

TABLE 1 Engine specifications

Make and Model	Peugeot 306 2.0L HDi
Year of Manufacture	2000
Number of Strokes	4-stroke
Number of Cylinders	4
Valvetrain	8 Valve, OHC
Static Compression Ratio	18:1
Engine Displacement [cc]	1997
Bore [mm]	85
Stroke [mm]	88
Connecting Rod Length [mm]	145
Intake Valve Diameter [mm]	35.6
Exhaust Valve Diameter [mm]	33.8
Intake Valve Opens (1mm lift)	170 CAD BBDC intake
Intake Valve Closes (1mm lift)	20 CAD ABDC intake
Exhaust Valve Opens (1mm lift)	45 CAD BBDC expansion
Exhaust Valve Closes (1mm lift)	10 CAD BTDC exhaust

the sensing tip. The junction is established by abrading the surface at 45° to the ribbons with a #400 grit emery cloth, such that several slivers form a connection between the two thermocouple metallic ribbons.

The testing session communicated in this paper was conducted with an oil temperature of 80°C±1°C at the sump. The oil used in this study was aged SAE 10W-40 API SN/CF, ACEA A3/B4, viscosity: 92.1 cSt @ 40°C and 14.4 cSt @ 100°C, both according to ASTM D445. In-cylinder pressure data was acquired after the coolant temperature was noted to have reached a natural thermal equilibrium with the oil at 80 °C.

Testing and Results

The aim of this paper was to test further the use of gases with high ratio of specific heats (γ) in the pressurized motored engine to vary the bulk gas temperature and monitor its effects on both the mechanical friction and heat transfer.

For mechanical friction testing, engine loading was kept constant at 103 bar while the engine speed and the ratio of specific heats were varied, which result in a change in bulk in-cylinder temperature. Table 2 shows the setpoints tested for FMEP determination.

For the determination of heat flux, eight setpoints were tested at two different engine speeds, two loading conditions and using pure Air and pure Argon. Table 3 shows the setpoints tested with the erodible E-type fast-response thermocouple fitted in the combustion chamber in place of the OEM injector.

TDC Determination

Obtaining the location of TDC with good accuracy enables the determination of the thermodynamic loss angle between the location of peak in-cylinder pressure (LPP) and TDC. An error of 1 DegCA in the TDC determination is reported to incur a 10 % error in the IMEP [8]. Good phasing between the pressure and volume data is always sought. In this study, prior undertaking the testing campaigns, an AVL TDC capacitive probe was used to measure the position of true TDC relative to the z-index (1 ppr) of the crankshaft encoder with a resolution of ±0.1 DegCA. Such testing was carried out on four different engine speed setpoints ranging from 1400 rpm to 3000 rpm, with the engine operating on Air as the working gas. It was found that the angular displacement between the z-index and TDC does not vary with engine speed. This angle was verified again after all the measurements reported in this work were obtained to ensure that no angular shifts between z-index and TDC were incurred during testing.

The FMEP determined in this work was obtained through an energy balance on the engine, explained by equation (1). Such method offers analytical simplicity, however the accuracy on the FMEP is dependent on the accuracy and resolution by which the IMEP and BMEP are obtained. The accuracy in obtaining the IMEP is dependent specifically on the measurement of in-cylinder pressure and phasing between the in-cylinder pressure and volume. In this regard, determining the FMEP from the pressurized motoring method renders the advantage that both the IMEP and BMEP are small in magnitude and comparable to the magnitude of the FMEP.

$$BMEP = \left(IMEP_{gross} + PMEP\right) - FMEP \quad (1)$$

Figure 2 shows the thermodynamic pressure loss angle at each setpoint tested. The thermodynamic loss angle is a measure of the heat and blow-by losses from the cylinder [9, 10]. The trend shown in Figure 2 is one which is expected, whereby the magnitude shows a decrease with an increase in engine speed due to less time per cycle allowed for heat and blow-by losses to flow out of the system. Increasing the ratio of specific heats resulted in an abrupt increase in thermodynamic loss angle up to γ of 1.6. Such observation is consistent with the expected increase in bulk in-cylinder temperature, driving a higher heat loss to the wall. The effect of blow-by on the thermodynamic pressure loss angle is hinted to have a

TABLE 2 Testing at 103 Bar for FMEP Determination

		Engine Speed [RPM]			
		1400	2000	2500	3000
Ratio of Specific Heats (γ)	1.40	✓	✓	✓	✓
	1.50	✓	✓	✓	✓
	1.60	✓	✓	✓	✓
	1.67	✓	✓	✓	✓

TABLE 3 Testing with erodible E-type fast-response thermocouple

		Engine Speed [RPM]			
		1400		2500	
Peak In-Cylinder Pressure [Bar]		80 bar	100 bar	80 bar	100 bar
Ratio of Specific Heats (γ)	1.40	✓	✓	✓	✓
	1.67	✓	✓	✓	✓

FIGURE 2 Graph of Pressure Loss Angle against Ratio of Specific Heats (γ)

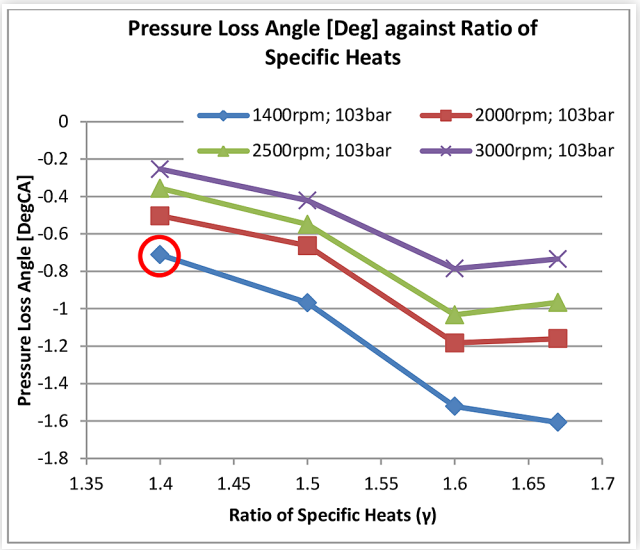

smaller effect than heat transfer [11]. From γ of 1.6 to 1.67, a decrease in pressure loss angle magnitude was noted. Such observation is consistent with that made in [5], however in this work, the magnitude decrease is more significant. Such observation might have resulted from several gas properties (such as density and thermal conductivity) imposing conflicting effects on the pressure loss angle. The thermodynamic pressure loss angle at 1400 rpm using air (encircled in Figure 2) was found to be -0.7 DegCA, which is a typical value for this speed and load testing regime.

Similar to the pressure loss angle, Figure 3 gives the loss angle between the computed peak gas in-cylinder temperature and the true TDC. It can be noted that the temperature loss angle is much larger in magnitude compared to each corresponding pressure loss angle, meaning that the peak in-cylinder temperature occurs before the peak in-cylinder pressure as shown in Figure 4 for the 1400 rpm, 103 bar setpoint using Air as the pressurization gas. This is discussed with reference to a T-s diagram by Pipitone [9] (Figure 2 given in [9]).

Computed and Measured Temperatures

Computing the bulk in-cylinder temperature from the measured pressure trace requires referencing of the in-cylinder pressure. Several pegging theories have been put forward by different authors [10, 12, 13], however one which has proved to give reliable results references the in-cylinder pressure at intake stroke to the measured MAP. It is thought that the best location during intake stroke to reference to the MAP is at the point where mass flow to the cylinder is small. This is to eliminate the effect of pressure losses through the poppet valves. Once proper referencing is obtained, equation (2) can then be used in a crank-resolved manner to compute the in-cylinder temperature at every crank angle increment during the valve-closed part of the cycle. T_{IVC} in equation (2) refers to the temperature of the bulk gas at intake valve closing. In this work, it was assumed that T_{IVC} is equal to the measured shunt pipe temperature at the intake side. The shunt pipe intake temperature was not controlled in this study, but left to reach a thermal equilibrium with the laboratory ambient temperature of around 21°C. The shunt pipe intake temperature is given in Figure 5, which shows that the variation in ratio of specific heats did not result in an appreciable change in the temperature of the re-circulated gas at the intake manifold. On the other hand, the engine speed seems to have had a strong effect on the re-circulated intake air temperature. This is however an expected result as an increase in engine speed allows less time for heat to flow out of the system.

FIGURE 3 The graph of Temperature Loss Angle against Ratio of Specific Heats (γ)

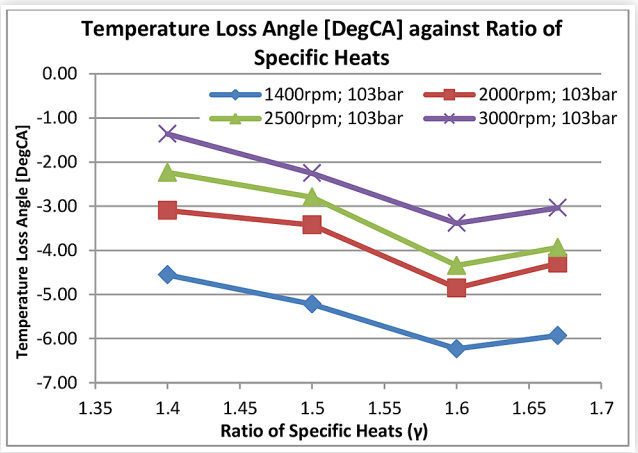

FIGURE 4 The graph showing angular difference between measured peak in-cylinder pressure and calculated peak bulk in-cylinder gas temperature for the setpoint of 1400 rpm, 103 bar using air as the pressurization gas.

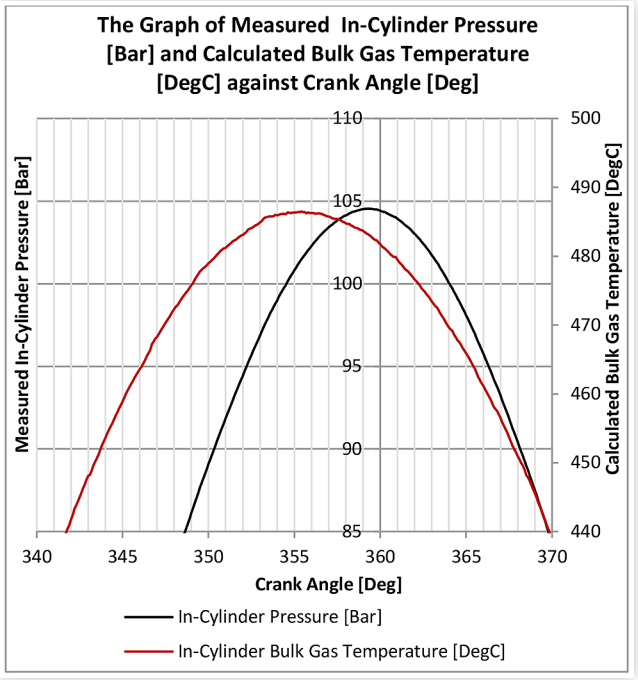

FIGURE 5 The graph of measured Intake Temperature against Ratio of Specific Heats (γ)

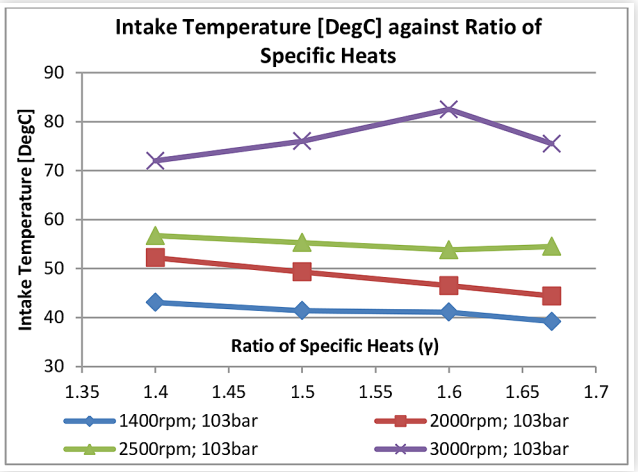

$$T(\vartheta) = T_{IVC}\frac{p(\vartheta)}{p_{IVC}}\frac{V(\vartheta)}{V_{IVC}} \quad (2)$$

Making use of equation (2) allows for an analytical evaluation of the bulk gas in-cylinder temperature as shown in Figure 6. It is evident that using gases of higher ratio of specific heats allow much higher bulk gas in-cylinder temperatures to be achieved. Figure 6 shows only the peak in-cylinder temperature for ease of comparison. These high in-cylinder temperatures are expected to allow for a better comparison of results between the pressurized motoring setup and the fired scenario.

Figure 7 shows the measured in-cylinder temperature through the ∅ 3 mm K-type thermocouple placed in the cylinder, protruding to around 1 mm from the piston top when at TDC. This graph gives neither the gas temperature, nor the metal surface temperature because of it being protruded from the combustion chamber surface by a few millimeters. Also, it should be mentioned that since this thermocouple is electrically isolated, the junction is situated behind a thin stainless steel body and encapsulated in magnesium-oxide. This however still gives an indication of the thermal differences in the cylinder induced by the gases with higher ratio of specific heats. From a pragmatic standpoint this measurement lies between the two other measured temperatures - oil/coolant temperature and the later presented gas-wall interface temperature.

FIGURE 6 The graph of Computed Bulk Gas Peak In-cylinder Temperature against Ratio of Specific Heats (γ)

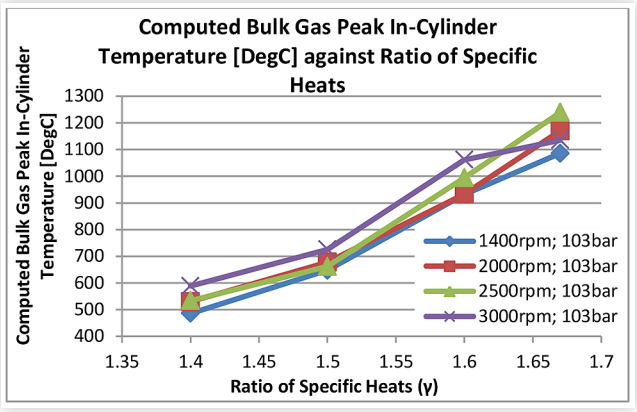

FIGURE 7 Measured In-cylinder Temperature (using ∅ 3 mm K-type thermocouple, protruding to 1mm from piston when at TDC) against Ratio of Specific Heats (γ)

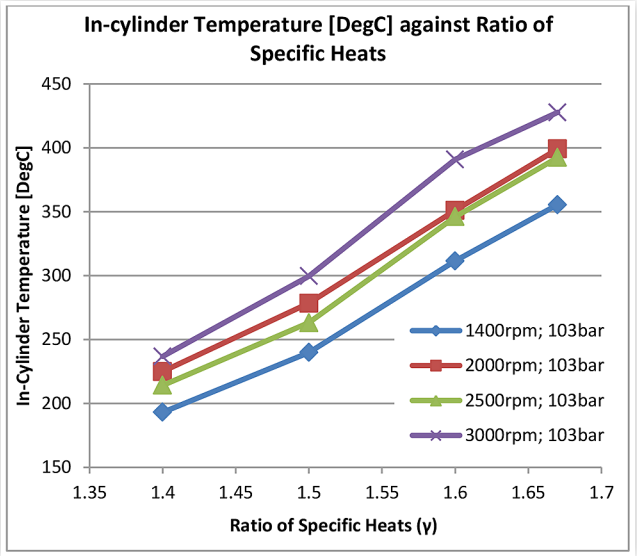

Effect of Ratio of Specific Heats on Manifold Absolute Pressure and PMEP

Obtaining a constant 103 bar with gases having different γ at different engine speeds required a different manifold pressure at every tested setpoint. This was obtained through two-stage mechanical regulation when supplying the engine from 200 bar gas cylinders. Only single-stage regulation was necessary for achieving stable manifold pressure when supplying air from a conventional 7 bar shop floor compressor. The manifold absolute pressure (MAP) required at each setpoint of engine speed and γ to obtain the 103 bar peak in-cylinder pressure is given in Figure 8. From this figure, it is evident that a drastic decrease in MAP was required with increasing the ratio of specific heats. Complementing such trend is the pumping mean effective pressure (PMEP) computed from the p-V indicator diagram. Figure 9 shows the PMEP for each setpoint tested.

One of the main criticisms of traditional pressurized motored testing is that the high peak in-cylinder pressures are reached at an expense of an abnormal increase in PMEP (resulting from the need of an increased MAP to achieve the required peak in-cylinder pressure), compared to the same condition in a fired engine [14, 15]. Figure 8 and Figure 9 show that using gases with high ratios of specific heats can result in high peak in-cylinder pressures, at a similar MAP and pumping effort to that in fired engines. In fact for the engine

FIGURE 8 The graph of Manifold Absolute Pressure against Ratio of Specific Heats for testing at 103bar peak in-cylinder pressure.

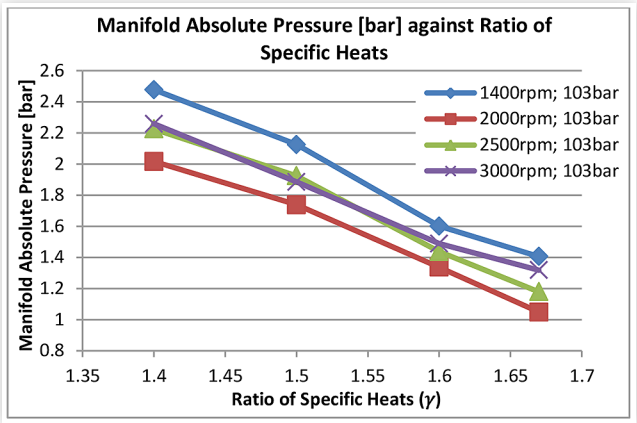

FIGURE 9 The graph of PMEP against Ratio of Specific Heats (γ)

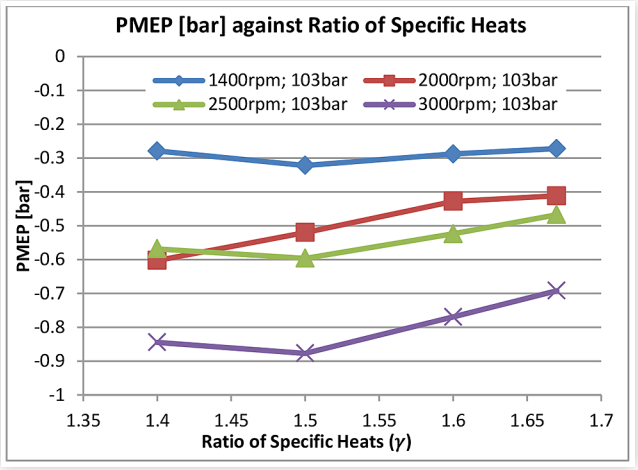

tested, at 3000 rpm, a peak fired cylinder pressure of 102 bar is measured with a MAP of 1.6 bar [3].

Blow-By

To approximate the blow-by mass flow out of the cylinder, the approach taken by Pipitone [9] was adopted, whereby the mass leakage is modeled as the gas flowing through an orifice. The orifice diameter was determined from 1D simulation performed in [16], where the diameter of the nozzle was varied until the simulation result of blow-by flow rate for all setpoints matched that which was experimentally obtained in [3]. The equivalent orifice diameter was found to be 0.6 mm.

In this work, the blow-by mass flow was computed on both the Air and Argon setpoints and it was found that the total mass escaped as blow-by per cycle is smaller for Argon compared to that for Air. Such result has to be seen in light of two properties which impose two conflicting effects. The ratio of specific heats, which is higher for Argon results in a higher flow-rate of blow-by. On the other hand, for two similar setpoints of engine speed and peak in-cylinder pressure, the in-cylinder pressure trace for Argon is smaller than that for Air throughout the whole 720 DegCA cycle, except for the peak in-cylinder pressure which is equal for both. This can be seen in Figure 10. Due to this global lower pressure for Argon, the potential for blow-by to flow out of the cylinder is less than that for an equivalent load setpoint using Air. This results mainly from the fact which was explained earlier that for an equal peak in-cylinder pressure, Argon requires a smaller value of MAP. This results in a total mass of gas leakage which is smaller for Argon than for Air at a similar setpoint. It should also be noted however that for a similar engine speed and peak in-cylinder pressure between Argon and Air, for the Argon case, a smaller initial trapped mass is evident. Due to this, the total blow-by mass escaping from the cylinder to the initial trapped mass, as a percentage, will be greater for Argon to that for Air for a similar setpoint. This is shown in Figure 11 for all setpoints of Air and Argon tested in this work.

FIGURE 10 The graph of in-cylinder pressure [bar] against crank angle [Deg]

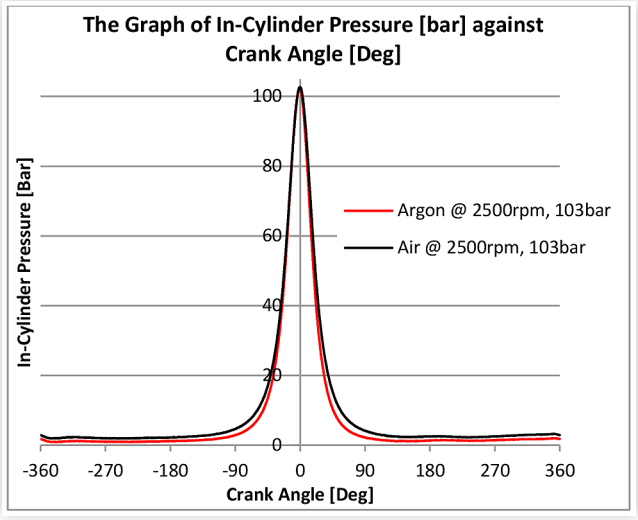

FIGURE 11 The graph of percentage total blow-by escaped to initial trapped mass [%] against engine speed [rpm]

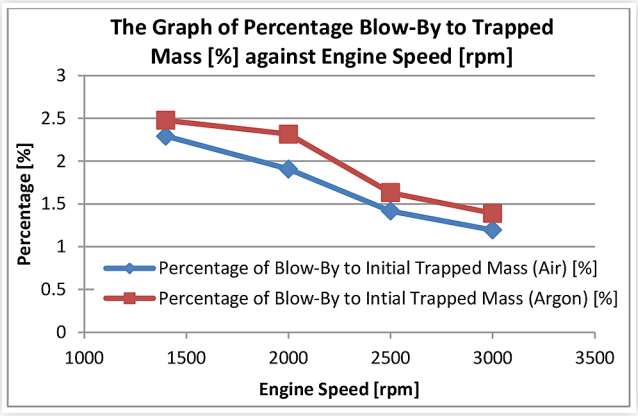

Indicated, Brake and Friction Mean Effective Pressures

The high bulk gas in-cylinder temperatures obtained in this study and shown in Figure 6 suggest a large magnitude of heat transfer out of the cylinder compared to conventional motoring using air. To evaluate this, the IMEP gross was plotted in Figure 12. It can be seen that between the case of pure Air and pure Argon, the losses in the form of heat flux and blow-by increased by a maximum of 67%. Such increase in losses originates largely from the heat transfer out of the cylinder, driven by the higher bulk in-cylinder temperatures.

Having obtained the IMEPgross, PMEP and measured the BMEP (shown in Figure 13), the FMEP could be computed using equation (1). Figure 14 shows the FMEP obtained in this study. It is evident that no measurable difference in the FMEP with γ was seen, except for three points which are thought to be outliers. These results confirm the findings of the previous work [5], where it was shown that using the pressurized

FIGURE 12 The graph of IMEPgross [bar] against Ratio of Specific Heats (γ)

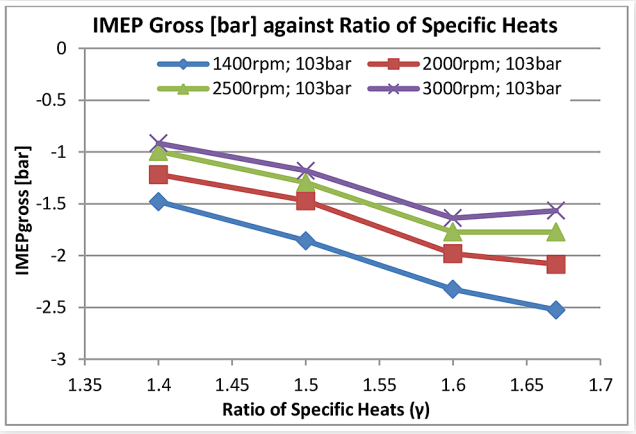

FIGURE 13 The graph of BMEP against Ratio of Specific Heats (γ)

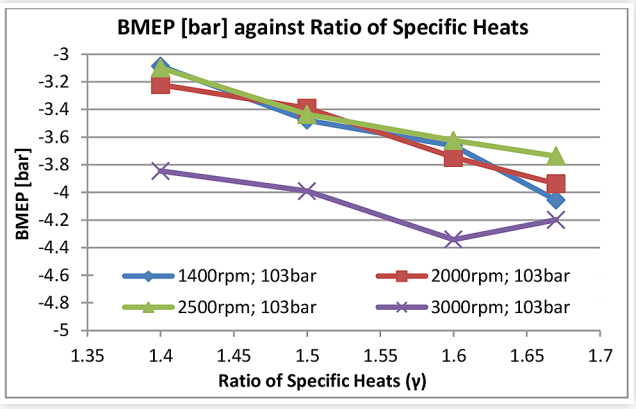

FIGURE 14 The graph of FMEP against Ratio of Specific Heats (γ)

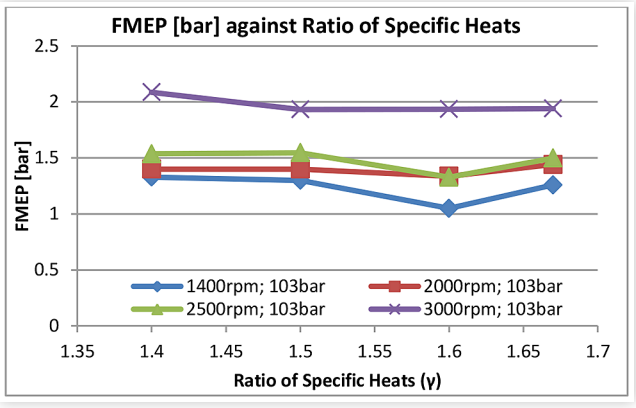

motoring method with higher in-cylinder temperatures rendered no measurable difference in the FMEP. Having presented this result, the authors would like to encourage further research on this modified pressurized motoring method, however from an instantaneous friction point of view, utilizing as an example the instantaneous IMEP method [17]. This would be able to provide data on whether the mechanisms of friction in the pressurized motoring method differ at elevated temperatures.

Having obtained more data with the modified pressurized motoring method, the authors are of the opinion, that even though no measurable difference in the FMEP was seen, using a gas with higher ratio of specific heats is still considered advantageous to achieve a fired-like pumping effort, as explained earlier in this work. This has to be seen from the aspect that using Argon and employing a blow-by recirculating compressor was found to be neither expensive nor very work-intensive to employ.

Gas-Wall Interface Temperature and Heat Flux

To understand further the effects of high in-cylinder temperatures in the motored engine, an erodible E-type, Nanmac fast-response thermocouple [18] was fitted in place of the OEM injector (as described in the Apparatus section). An adaptor made out of aluminum was manufactured to be able to fit the 1/8" thermocouple in the aluminum cylinder head. Figure 15 shows the E-type thermocouple fitted in the machined adaptor, whereas Figure 16 shows the erodible thermocouple fitted in the combustion chamber of the 2.0L HDi engine cylinder head, where the thermocouple is flush with the head surface, i.e. does not protrude into the combustion chamber.

Erodible thermocouples have been relatively popular in the area of heat transfer studies, mainly because it is one of the only few neat solutions of how the rapidly changing gas-wall interface temperature can be measured without large physical disturbance to the in-cylinder conditions. Computing the heat flux from these thermocouples requires a one-dimensional heat flux assumption, which has been criticized by several authors, to name a couple [19, 20]. It has been also agreed however that no other viable method yet exists [20], which offers better alternative to the measurement of instantaneous gas-wall interface heat flux. In this work, the use of this thermocouple was mainly aimed at estimating the difference in thermal conditions at the gas-wall interface exhibited between using air and argon as the pressurization gases. This is being pointed out as it is known and acknowledged that several factors which yet remain unknown affect the accuracy of gas-wall interface temperature and heat flux determination. Some of these factors include the one-dimensional assumption which is largely untrue. Another limitation includes the difficulty of determining which material affects mostly the transient heat transfer, whether the mica sheets between the two

FIGURE 15 The erodible E-type thermocouple fitted in the machined Aluminum adaptor

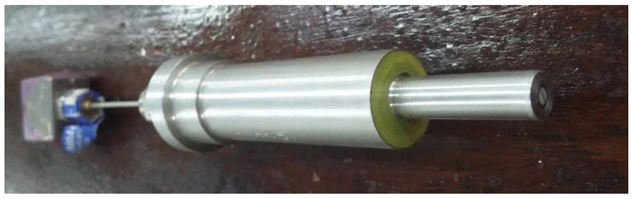

FIGURE 16 The erodible E-type thermocouple fitted flush with cylinder head surface

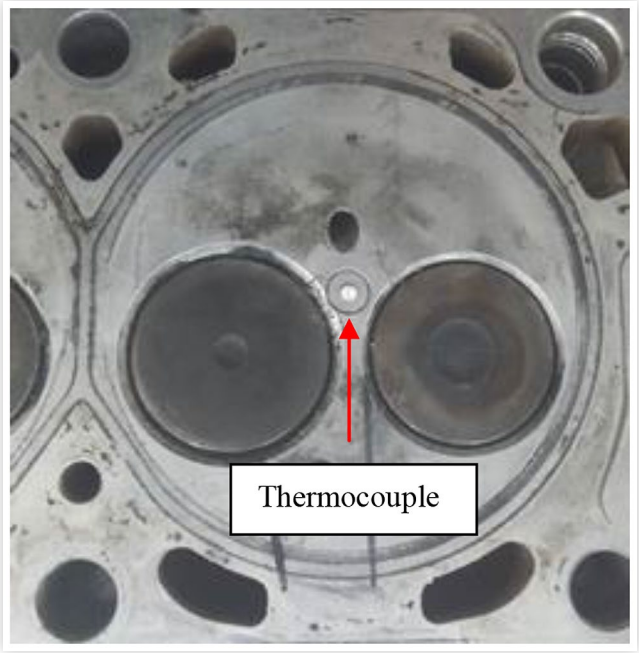

FIGURE 17 Microscope image of the E-type erodible thermocouple

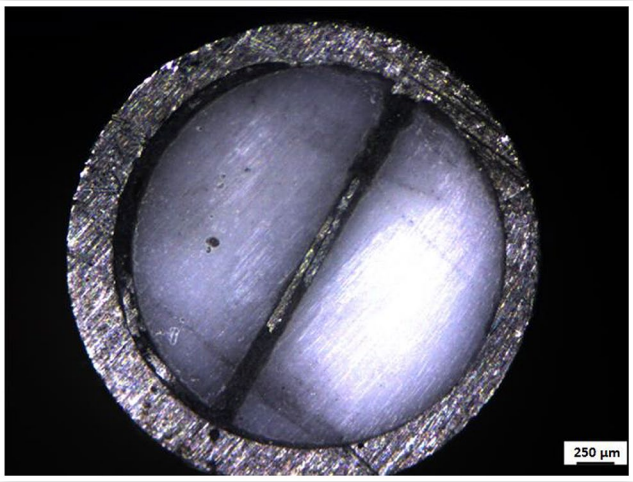

FIGURE 18 The graph of ensemble gas-wall interface temperature and ensemble heat flux at 1400 rpm, 103 bar using pure Air as the pressurization gas

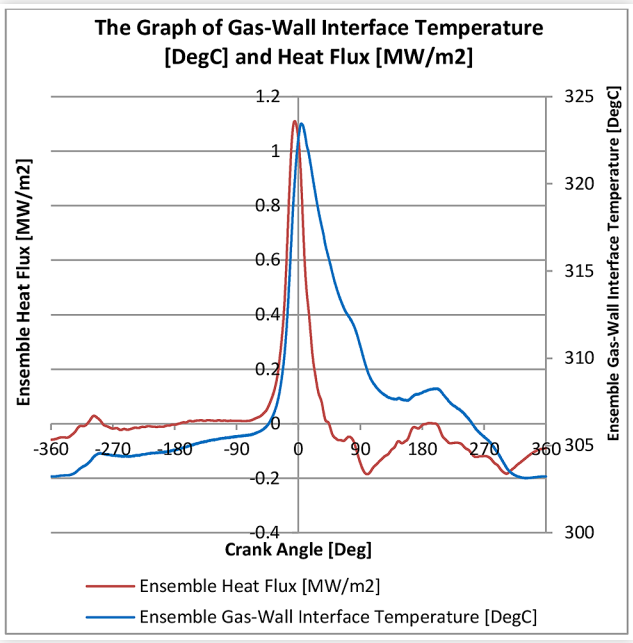

thermocouple ribbons, the zirconia split-tapered inserts, the stainless steel body of the thermocouple or the aluminum adaptor/cylinder head. Such difficulty remains without an answer. It has been also reported that different locations at the combustion chamber surface are affected with different magnitudes of heat flux, this being mainly due to different flow regimes. In this study, the erodible thermocouple location of installation was constrained by the injector position, which is situated between the intake and exhaust valves as seen in Figure 16. A further limitation on heat flux determination includes the effect of oil deposits in the motored engine on the thermocouple junction, which slows down the response of the temperature reading [21]. Knowing that the injector housing in the cylinder head passes through the coolant jacket, it is also thought that the 'stem effect' described by Nanmac [22] and the 'fin effect' described by Farrugia [23] might induce some error on the heat flux determination. Figure 17 shows a microscope image of the composition of the erodible thermocouple used in this study, together with an appropriate scale bar.

The mentioned factors all contribute to a somewhat questionable heat flux being determined from gas-wall interface temperature measurements. It is however still deemed important to have some knowledge of what could be happening in the motored engine with increasing the bulk gas temperature. Figure 18 and Figure 19 show the gas-wall interface temperature and heat flux traces acquired at 1400 rpm using pure air and pure argon respectively as the pressurization gas. These were taken at 103 bar peak in-cylinder pressure. The shape and characteristics of these graphs are representative of all setpoints tested. It can be seen that the usual peculiarities of the transient heat flux are visible in such traces, mainly the peak heat flux occurring prior to the peak gas-wall interface temperature and the rapid decline in heat flux and even changing direction not long after TDC. Such phenomena have been reported by researchers, such as Nijeweme [24]. In comparing these traces with those obtained from other studies, it should be kept in mind that heat flux probes give a local measurement and different locations on the cylinder head surface may have different heat flow conditions.

In comparing Figure 18 and Figure 19, it can also be noted that the gas-wall interface temperature between air and argon has a slightly different characteristic after TDC. The temperature for air falls much more rapidly than that for argon. It should be pointed out that the thermal capacity of the sliver formed by the abrasive action on the E-type thermocouple to some extent has an effect on the response of the thermocouple.

FIGURE 19 The graph of ensemble gas-wall interface temperature and ensemble heat flux at 1400rpm, 103bar using pure Argon as the pressurization gas

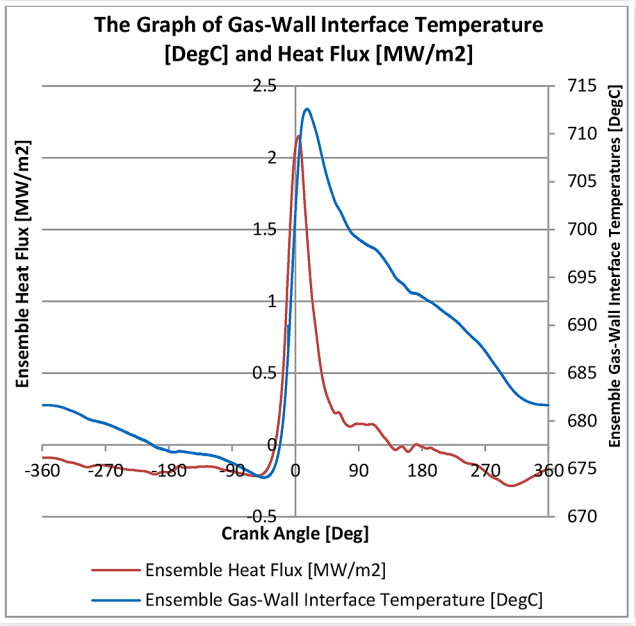

FIGURE 20 A graph comparing the scales of oil temperature, k-type thermocouple temperature, gas-wall interface temperature and calculated bulk-gas temperature at 1400 rpm, 103 bar using Air.

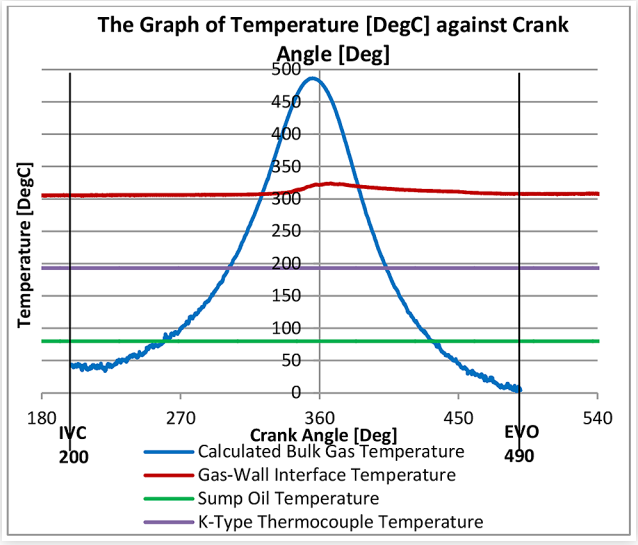

Due to this, it is unsure whether the two measurements showing the different transient nature of the gas-wall interface temperature between Air and Argon is potentially affected by a different thermal capacity of the junction of the thermocouple.

Table 4 gives the computed average of the measured gas-wall interface temperatures. The gas-wall interface temperature is defined by Nanmac [7] as being the temperature of the gases beneath the laminar layer formed at the wall surface [21]. A drastic increase with an average of 68% was noted in gas-wall interface temperature between tests done with air and those with argon. Figure 20 shows a graph for the valve-closed part of the cycle comparing the magnitudes of the cylinder-related temperatures, measured or calculated in this work. This figure also shows the relative difference in the swing between that for the calculated bulk gas temperature and that for the gas-wall interface temperature. The K-type thermocouple measured temperature is also shown to lie between the temperature of the oil measured at the sump, and that for the gas-wall interface temperature.

To have a benchmark comparison of heat flux, the average of the transient component of heat flux was computed on the valve-closed part of the cycle and given in Table 5. It should be said that in the determination of the transient heat flux magnitude, the thermal properties of Zirconia as given by Nanmac (k @ 800 °C: 2 W/mK, ρ: 5.7 g/cc, α: 7.29x10^{-7} m^2/s) were used. Since Zirconia has a thermal conductivity of around seven times smaller than that of stainless steel (making up the thermocouple body) and around one hundred times smaller than that of Aluminum (making up the cylinder head), it is said by Nanmac that the temperatures being measured can be classified as being equal to the gas found behind the laminar layer at the wall-surface [7].

In several heat flux studies, thermocouples recessed from the cylinder head surface were used to determine also the steady-state portion of the heat flux between the fast response thermocouple and the recessed thermocouple, making use of Fourier's 1D conduction equation. It should be noted that in this study, a recessed thermocouple was not used. Hence the values of heat flux given in this work, as computed from the E-type thermocouple, give only the transient component of heat flux. It can be seen in Figure 18 and Figure 19 that around compression TDC, the instantaneous heat flux goes to Megawatts/m^2 (MW/m^2) values. It should be noted however,

TABLE 4 The average in-cylinder gas-wall temperatures computed from the measured fast-response thermocouple

Average Gas-Wall Interface Temperature [DegC]			Engine Speed [rpm]	
			1400	2500
Peak In-Cylinder Pressure	80 bar	Air	298	321
		Argon	661	725
	100 bar	Air	307	335
		Argon	686	787

TABLE 5 Average heat flux computed through temperature measurements from the erodible thermocouple

Average Heat Flux [kW/m^2]			Engine Speed [rpm]	
Average Heat Transfer [kW]			1400	2500
Peak In-Cylinder Pressure	80 bar	Air	79.71	109.94
			0.77	*1.08*
		Argon	324.51	235.84
			3.64	*2.27*
	100 bar	Air	104.50	137.03
			1.02	*1.26*
		Argon	246.28	226.94
			2.80	*2.00*

that such high magnitudes last for very short crank angle durations, especially in this study since the engine is motored. Computing the average over the whole cycle therefore results in much smaller magnitudes synonymous to the kilowatts/m^2 (kW/m^2) order as seen in Table 5. Table 5 also shows the average heat transfer (kW), taking into account the area of the combustion chamber, piston surface and swept area of the wall. It is noted that when the transient component of the heat transfer obtained from the eroding surface thermocouple was compared with that obtained from the first law of thermodynamics on the valve-closed part of the cycle (between IVC 160 DegCA BTDC and EVO 130 DegCA ATDC), the average from the eroding surface thermocouple was found to be relatively smaller than that of the first law. Such difference can be attributed to the fact that the heat flux being measured is mainly affected by the Zirconia split-tapered inserts. Zirconia is a very insulative material and hence a smaller heat flux is measured since the rest of the combustion chamber is made from a much more conductive material, being aluminum. Due to this, the measurement of heat flux as obtained in this work was subjected to the opposite of what is termed 'the fin/stem effect' [22, 23]. To have a comparison between heat flux determined from the first law and that obtained from the eroding thermocouple, Figure 21 was plotted, showing both traces for the 2500 rpm, 84 bar using air as the pressurization gas. It should be said that the trace for the first law shown in Figure 21 is very similar to that reported in [16] for the setpoint of 3000 rpm, 84 bar air conducted on the same engine being studied in this work. It can be seen from Figure 21 that the peak heat flux from the first law occurs earlier than that obtained from the thermocouple. This shift might be a result of the heat capacity of the Zirconia and the thermocouple junction. Another difference seen between the two traces is the earlier transition to negative heat flux as obtained from the first law, compared to that from the thermocouple. Such difference is also thought to have originated from the heat capacity of the thermocouple.

FIGURE 21 The graph comparing the heat transfer obtained from the first law of thermodynamics and the transient component of heat transfer obtained from the E-type eroding thermocouple

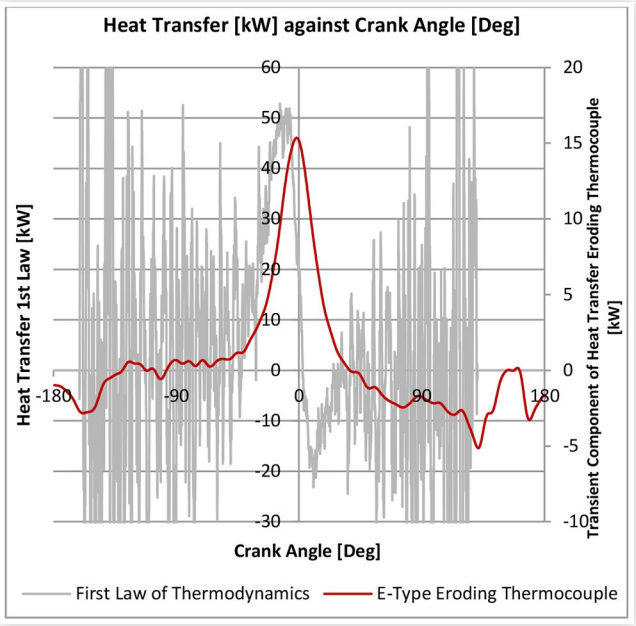

Discussion

The FMEP obtained from pressurized motoring testing has been criticized several times on the criteria that the in-cylinder temperatures are not representative of the true fired scenario which might in turn induce a higher friction footprint due to the higher oil viscosity [14, 25]. It was also stated that thermal expansions might be less, which on the other hand promotes a lower friction prediction. Richardson [14] explained how the first compression ring might be subjected to a boundary lubrication condition in firing, but not so in pressurized motoring. At large, some authors agree that the conventional pressurized motoring using air and fired engines have several differences in the mechanical friction mechanisms which when coupled together gives an overall comparable FMEP magnitude. To address this criticism, in this study, the relationship between bulk in-cylinder temperature and FMEP was studied. It was shown that for the pressurized motoring method, an increase in bulk in-cylinder temperature results in no measurable difference in the FMEP. This conclusion is consistent with that reported in [5], for a smaller engine loading condition of 84 bar, same engine speeds of 1400rpm - 3000rpm and same ratio of specific heats 1.4, 1.5, 1.6 and 1.67.

Another criticism for the conventional pressurized motored method regards the higher PMEP induced in pressurized motoring due to the higher manifold pressure that has to be imposed to reach the fired-like in-cylinder pressures. This study addresses this limitation and has shown that using gases of high γ results in fired-like peak in-cylinder pressures without a need for an excessive manifold pressure, and abnormal increase in PMEP.

Apart from the versatility of using the pressurized motoring method for FMEP measurements, having a reliable heat flux measurement in such setup gives an added possibility of understanding the heat transfer from a more fundamental point of view in which the complications associated with combustion are removed. Furthermore, the suggested modification of using gases other than air allows the determination of heat flux independent of the conventional air-fossil fuel system. A study carried out by Demuynck [26] used a motored engine at relatively low speeds and low compression ratio, in which Argon, Helium and CO_2 were injected in the cylinder to develop correlations of how the heat transfer varies with respect to the dynamic viscosity, density, heat capacity, thermal conductivity and Prandtl number of the gas. Such study was aimed at developing a correlation between the mentioned variables in the hope of developing a fuel-independent heat transfer model. The most standing conclusion from this study carried out by Demuynck [26] is that having a gas with a high dynamic viscosity, such as Argon, affects the heat transfer in two contrasting ways; an increase in heat

transfer due to the higher temperatures at the end of the compression stroke, but also a decrease in heat transfer due to a decreased convective heat transfer coefficient.

It was said earlier that the heat flux results reported in this work which were obtained from the eroding thermocouple give only the transient component of heat flux. It should be said that if Zirconia is the dominant material for heat flow, the distance from the cylinder head surface at which the recessed thermocouple should be placed to measure an attenuation of 0.5 % of the temperature swing is 0.75 mm for the lowest engine speed of 1400 rpm tested in this work. The lowest engine speed is considered in this calculation because heat flow will penetrate the furthest at the lower engine speeds [23]. The 0.75 mm recessed distance for Zirconia is small compared to 1.6 mm for Stainless Steel and 7 mm for Aluminum. It can therefore be said that had this recessed thermocouple been implemented, the assumption of 1D from the surface to the coolant jacket (i.e. along the axis of the Zirconia split-tapered inserts) would have been a better assumption compared to that if made on Stainless Steel or Aluminum. It is thought that since Zirconia requires a small recessed distance, the temperature of the stainless steel pipe surrounding the Zirconia can be measured and used as the recessed temperature for the determination of the steady heat flux component. This proposition however suggests that the majority of the heat flows radially from the junction of the thermocouple, and not axially. This argument might be justified due to the fact that radially, the distance between the junction and the nearest heat sink, being the stainless steel tube is equal to the radius of the Zirconia (Figure 17) and hence smaller than the axial distance to the nearest heat sink, being the full length of the Zirconia split-tapered inserts.

It has been shown that utilizing gases of high ratios of specific heat induces bulk in-cylinder temperatures comparable to firing. This addresses the criticism of thermal expansion and oil viscosities. It can be seen that with the high bulk temperatures achieved in this study, the fired engine is better represented. It is however still pointed out that with any motored setup, the peak in-cylinder pressure still occurs at around 1 DegCA BTDC, whereas in fired engines, this occurs at around 10 DegCA ATDC. This difference in the location of peak in-cylinder pressure changes the dynamics of how the in-cylinder temperature affects the FMEP. Having a high in-cylinder temperature and peak in-cylinder pressure at around 1 DegCA BTDC has a high degree of probability that boundary friction dominates due to the piston being virtually at rest. On the other hand, at around 10 DegCA ATDC, the piston speed would already have increased appreciably, meaning that a greater degree of hydrodynamic lubrication is possible. Another factor which differs between the two situations is the connecting rod angle which plays an important role in the normal reaction which promotes rubbing between the piston skirt and the cylinder wall. At 1 DegCA BTDC, the connecting rod is virtually vertical, hence minimal normal reaction, whereas at 10 DegCA ATDC, the normal reaction magnitude would already have increased appreciably. This means that although the authors promote the idea of using gases of higher ratios of specific heats, it is still realized that a difference between the fired and motored engine testing exists. On the other hand however, one has to consider that at present times, this method is in competition with tests such as the teardown, hot coasting, Morse test and fired indicating (IMEP) method, amongst which the teardown seems to be the most popular with OEMs. It has been proved by some authors [14] that these methods have significant limitations, such as isolating the FMEP from engine loading, FMEP not measured at thermal steady-state conditions, interaction of the FMEP of several components not taken into account, disadvantage of having to take apart the engine rather than testing as a whole, high magnitudes of numerical error propagation, etc. It is also worth mentioning that the limitation imposed by the peak in-cylinder pressure timing is offset by the higher level of accuracy/repeatability of this method. A one-dimensional model can be tuned to a pressurized motoring scenario (exploiting its accuracy/repeatability) and then the model will have to bridge a smaller gap from motoring to firing condition. Therefore, this study aims to communicate both the capabilities and limitations of the modified version of the pressurized motored method, in the hope of promoting its use amongst OEMs and other research institutes.

Accurate and physically representative mathematical friction models are required for the production engine. These friction models have uses, such as, for virtual torque estimation in the control of the engine (ECU), or vehicle level simulations for fuel economy/emissions optimization e.g. the power split optimization between the internal combustion engine and the electrical drive in a hybrid vehicle.

In general, such engine friction models are based on a "teardown" motoring test which have the necessary consistency/repeatability but lack the load sensitivity. Vice versa engine friction models based on fired tests fall short on the consistency /repeatability but add a degree of granularity for engine load. When faced with such a dilemma it is proposed here to use the pressurized motored test since it benefits from consistency, repeatability and also includes the load sensitivity.

Table 6 shows a comparison between the ratio of FMEP to BMEP for fired and motored tests published in [3] and in this work. It shows that for a given setpoint of 3000 rpm, 102 - 103 bar, the FMEPs are similar to each other for both testing methods. The difference lies with FMEP/BMEP ratio, which is an indicator of the robustness of the FMEP measurement, only 16 % for the fired case and around 46 % to 55 % for the pressurized motored case. This shows that the pressurized motored method accentuates the friction portion from the total losses measurement by more than three fold.

Pressurized motoring can be a viable (cheap/accurate/repeatable) method for friction determination of stabilizing engines intended for fuel economy tests or other elaborate testing. It might provide an early indication of, among other things, anomalies in the friction of the rotating assembly without pressure indication measurement. When pressure indicating measurement is used, more detailed friction measurement can be obtained, but other vital health checks can be made for blow-by, theoretical versus “true”/dynamic compression ratio, etc. It is appreciated that this might require a “break” in the build phase of the prototype production engine (to attach a shunt pipe instead of, say, the turbo) but after the pressurized motoring test and the rest of the engine build is complete, the engine is ready for the more intensive/costly fired testing (e.g. fuel economy). The cost of the “extra” motoring

TABLE 6 Comparison of FMEP/BMEP sensitivity between fired and motored testing (at 3000 rpm)

Method	Peak In-Cylinder Pressure [bar]	Working Fluid	BMEP [bar]	FMEP [bar]	$\frac{FMEP}{BMEP} \times 100$ (absolute)
Fired 1.6bar MAP*	102	Air/Fuel	11.40	1.80	15.8 %
Motored †	103	Air	- 3.85	2.09	54.3 %
Motored †	103	Argon	- 4.20	1.94	46.2 %

* Data published in [3], Table 4
† Data shown in Figure 13 and Figure 14 in this publication

test is expected to be outweighed by the savings from the more expensive fired test - less delays, etc. The energy requirements, and therefore the associated hardware costs, to motor the engine is quite low even at rated peak cylinder pressures - a fact that can be leveraged in the experimentalist's favor.

Conclusions

Mechanical engine friction and heat transfer from the cylinder are two main parasitic losses which had been researched for several decades. Despite this, reliable experimental data is still sought, mainly to aid in engine design and modeling. Modern engines are subjected to higher engine speeds, higher compression ratios, different fuels, etc. Due to this, new experimental data is required to calibrate existing engine models to new engine designs.

The pressurized motoring method has been found to offer reliable measurements at moderate testing cost. A modification to the conventional motoring method is put forward, where instead of using Air, gases of higher ratios of specific heat are used to pressurize the engine. This was found to address two main limiting factors of the pressurized motoring method. Such modification was found to successfully increase the in-cylinder temperatures to values synonymous to the fired engine. Also, the pumping work and manifold pressure required to achieve fired-like peak in-cylinder pressures were found to be similar to that in a fired engine if gases with high ratio of specific heats are used as the pressurization gas.

An eroding thermocouple has been used to give an indication of the gas-wall interface temperature which results from testing with high ratios of specific heat. An average increase of around 400°C in gas-wall interface temperature and an increase of around 600°C in the calculated peak in-cylinder gas temperatures were noted between setpoints tested with pure Air and pure Argon.

The FMEP as determined from the IMEP and BMEP was found to show no measurable difference for testing with different ratios of specific heats. This means that the determination of FMEP from pressurized motoring method is insensitive to the in-cylinder temperatures. Such result confirms the conclusion made in [5] for testing at a lower peak in-cylinder pressure of 84 bar. It was also shown that using gases with higher ratio of specific heats gives the test a more fired-like footprint due to having a more representative PMEP, hence the experimentalist using the Pressurized motoring can favor Argon testing because it bridges the gap between motoring and firing both from thermal loading and pumping effort.

References

1. Knauder, C., Allmaier, H., Salhofer, S., and Sams, T., "The Impact of Running-In on the Friction of an Automotive Gasoline Engine and in Particular on Its Piston Assembly and Valve Train," *Proceedings of the Institution of Mechanical Engineers, Part J: Journal of Engineering Tribology* 232(6):749-756, 2017.
2. Pike, W.C. and Spillman, D.T., "The Use of a Motored Engine to Study Piston-Ring Wear and Engine Friction," *Proceedings of the Institution of Mechanical Engineers* 178(14):37-44, 1963.
3. Caruana, C., Farrugia, M., and Sammut, G., "The Determination of Motored Engine Friction by Use of Pressurized 'Shunt' Pipe between Exhaust and Intake Manifolds," SAE Technical Paper 2018-01-0121, 2018, https://doi.org/10.4271/2018-01-0121.
4. Caruana, C., Farrugia, M., Sammut, G., and Pipitone, E., "Further Experimental Investigation of Motored Engine Friction Using Shunt Pipe Method," SAE Technical Paper 2019-01-0930, 2019, https://doi.org/10.4271/2019-01-0930.
5. Caruana, C., Farrugia, M., Sammut, G., and Pipitone, E., "Experimental Investigation on the Use of Argon to Improve FMEP Determination through Motoring Method," SAE Technical Paper 2019-24-0141, 2019, https://doi.org/10.4271/2019-24-0141.
6. "Nanmac High Performance Thermocouples," https://dl.airtable.com/.attachments/e9338953b17122077ebff9a29bb5ad23/a0ec6abf/Corporate_Capabilities_Presentation_Jan_2016.pdf.
7. Nanigian, J. and Nanigian, D., "A Unique Thermocouple Used to Measure: Squibs, Ignitors, Propellants, and Rocket Nozzles," *Nanmac Holliston*. https://dl.airtable.com/.attachments/00993a07cca1d6b969c6dfb2b66431a2/ac50042b/eroding-thermocouple.pdf.
8. Pipitone, E., Beccari, A., and Beccari, S., "The Experimental Validation of a New Thermodynamic Method for TDC Determination," SAE Technical Paper 2007-24-0052, 2007, https://doi.org/10.4271/2007-24-0052.
9. Pipitone, E. and Beccari, A., "Determination of TDC in Internal Combustion Engines by a Newly Developed Thermodynamic Approach," *Applied Thermal Engineering* 30:1914-1926, 2010.

10. Davis, R. and Patterson, G., "Cylinder Pressure Data Quality Checks and Procedures to Maximize Data Accuracy," SAE Technical Paper 2006-01-1346, 2006, https://doi.org/10.4271/2006-01-1346.
11. Tunestal, P., "Model Based TDC Offset Estimation from Motored Cylinder Pressure Data," in *Proceedings of the 2009 IFAC Workshop on Engine and Powertrain Control, Simulation and Modeling, Rueil-Malmaison*, France, Nov 30-Dec 2 2009, 241-247.
12. Gopujkar, S., Worm, J., and Robinette, D., "Methods of Pegging Cylinder Pressure to Maximize Data Quality," SAE Technical Paper 2019-01-0721, 2019, https://doi.org/10.4271/2019-01-0721.
13. Randolph, A., "Methods of Processing Cylinder-Pressure Transducer Signals to Maximize Data Accuracy," SAE Technical Paper 900170, 1990, https://doi.org/10.4271/900170.
14. Richardson, D.E., "Review of Power Cylinder Friction for Diesel Engines," *Transactions of the ASME* 122, 2000.
15. Kovach, J., Tsakiris, E., and Wong, L., "Engine Friction Reduction for Improved Fuel Economy," SAE Technical Paper 820085, 1982, https://doi.org/10.4271/820085.
16. Caruana, C., Farrugia, M., Sammut, G., and Pipitone, E., "One-Dimensional Simulation of the Pressurized Motoring Method: Friction, Blow-by, Temperatures and Heat Transfer Analysis," in *Internal Combustion Engines and Powertrain Systems for Future Transport*, West Midlands, December 11-12, 2019.
17. Uras, H. and Patterson, D., "Measurement of Piston and Ring Assembly Friction Instantaneous IMEP Method," SAE Technical Paper 830416, 1983, https://doi.org/10.4271/830416.
18. "Eroding Junction Thermocouple - Maintenance," Nanmac, Holliston.
19. Buttsworth, D.R., Stevens, R., and Stone, R.C., "Eroding Ribbon Thermocouples: Impulse Response and Transient Heat Flux Analysis," *Measurement Science and Technology*, 2005.
20. Hendricks, T. and Ghandhi, J., "Estimation of Surface Heat Flux in IC Engines Using Temperature Measurements: Processing Code Effects," *SAE Int. J. Engines* 5(3):1268-1285, 2012, https://doi.org/10.4271/2012-01-1208.
21. Dao, K., Uyehara, O., and Myers, P., "Heat Transfer Rates at Gas-Wall Interfaces in Motored Piston Engine," SAE Technical Paper 730632, 1973, https://doi.org/10.4271/730632.
22. "The Stem Effect: Leading Cause of Error in Temperature Measurement," Nanmac, Holliston, Massachusetts.
23. Farrugia, M., *Transient Surface Heat Flux Measurements in a Straight Pipe Extension of the Exhaust Port of a Spark Ignition Engine* (Michigan: Oakland University, 2005).
24. Nijeweme, D.J.O., Kok, J.B.W., Stone, C.R., and Wyszynski, L., "Unsteady In-Cylinder Heat Transfer in a Spark Ignition Engine: Experiments and Modelling," *Proceedings of the Institution of Mechanical Engineers, Part D: Journal of Automobile Engineering* 215:747-760, 2001.
25. Mauke, D., Dolt, R., Stadler, J., Huttinger, K., and Bargende, M., *Methods of Measuring Friction under Motored Conditions with External Charging* (Switzerland: Kistler Group, 2016).
26. Demuynck, J., De Paepe, M., Sileghem, L., Vancoillie, J. et al., "Applying Design of Experiments to Determine the Effect of Gas Properties on In-Cylinder Heat Flux in a Motored SI Engine," *SAE Int. J. Engines* 5(3):1286-1299, 2012, https://doi.org/10.4271/2012-01-1209.

Contact Information

Mario Farrugia, Mechanical Engineering Department, University of Malta, Malta
mario.a.farrugia@um.edu.mt

Carl Caruana, Mechanical Engineering Department, University of Malta, Malta.
carl.caruana.12@um.edu.mt

Acknowledgments

The authors express their sincere gratitude to Continental Corporations for the donation of the UniNOx sensor used to verify gas mixtures. Methode Electronics Malta are thanked for the donation of the data acquisition system. Ing. Noel Balzan, Ing. Jean Paul Azzopardi and Mr. Andrew Briffa are thanked for their help throughout this project.

The research work disclosed in this publication is partially funded by the Endeavour Scholarship Scheme (Malta). Scholarships are part-financed by the European Union-European Social Fund (ESF)-Operational Programme II-Cohesion Policy 2014-2020 "Investing in human capital to create more opportunities and promote the well-being of society".

Definitions/Abbreviations

AC - Alternating Current
ATDC - After Top Dead Centre
BBDC - Before Bottom Dead Centre
BDC - Bottom Dead Centre
BMEP - Brake Mean Effective Pressure
BTDC - Before Top Dead Centre
CA - Crank Angle
CAD - Crank Angle Degrees
CI - Compression Ignition
EVO - Exhaust Valve Opened
FMEP - Friction Mean Effective Pressure
HDi - High-Pressure Direct Injection
IMEP - Indicated Mean Effective Pressure
IVC - Intake Valve Closed
LPP - Location of Peak Pressure
MAP - Manifold Absolute Pressure
OEM - Original Equipment Manufacturer
PMEP - Pumping Mean Effective Pressure
ppr - Pulse Per Revolution
TDC - Top Dead Centre
VFD - Variable Frequency Drive

Appendix

In the photograph shown below, all sensors are aligned in their axial sealing location so that an observation on the protruding length could be made, i.e. the eroding thermocouple is the shortest because its end is flush with the cylinder head. The injector slightly protrudes into the combustion chamber, while TDC probe is the longest as it needs to be very close to the piston top for proper measurement. The K-type thermocouple was protruded to a length slightly shorter to that of the TDC probe.

FIGURE 22 Photograph of (starting from the top) the E-type Eroding thermocouple, TDC probe, K-type thermocouple and OEM injector, all of which are mountable in the injector hole in the cylinder head.

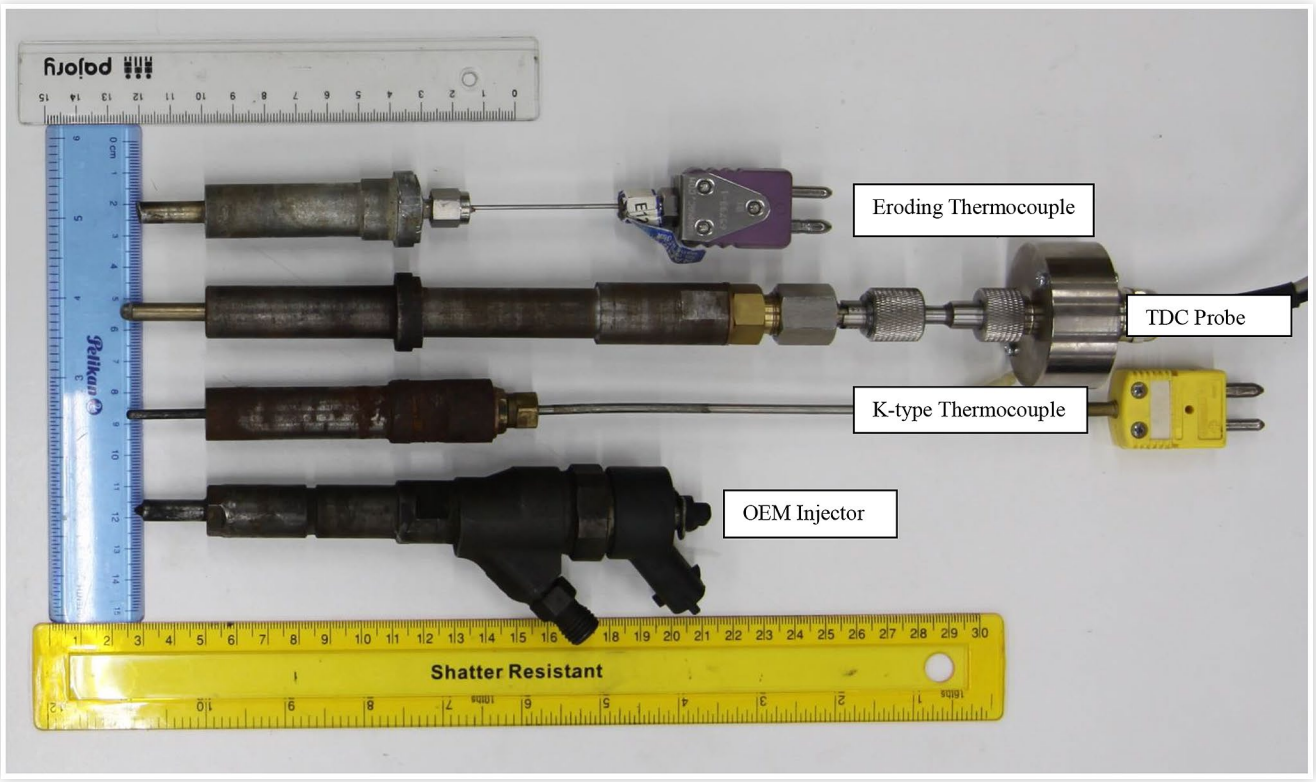

e-ISSN 2641-9645